

Numerical and Heat Transfer Analysis of Shell and Tube Heat Exchanger with CUO as NANO Fluid

S.Prasad

Department of Mechanical
Engineering,
AITAM College, India.

Dr.N.Haribabu

Department of Mechanical
Engineering,
AITAM College, JNTUK, India.

M.Venkata Ramana

Department of Mechanical
Engineering,
AITAM College, India.

ABSTRACT:

Shell and Tube Heat Exchanger (STHE) has its own importance in the industrial applications. The improvement of efficiency of the STHE using different design modifications in the shell side and different concentrations of Nano fluids results in increase of overall efficiency. In that view, Experimental and numerical simulations are carried for a single shell and multiple pass heat exchanger with different baffle cuts. The experiment was carried out with hot fluid as a water in tube side and cold fluid as a water in shell side with circular tubes at 60° tube orientation and 25% baffle cut. Heat transfer rates and pressure drops are calculated for various Reynolds numbers from 4000 to 20000. Fluent software is used for numerical investigations. Both water and different concentrations i.e. 0.1%, 0.4%, 0.8% of CuO are used for the numerical studies. In addition to 25% baffle cut, quarter baffle cut and mirror quarter baffle cut arrangements are used for comparison. The experimental values of heat transfer rates and pressure drops over shell side and tube side along the length of STHE are compared with those obtained from fluent software. It is found that the CuO 0.8% concentration Nano fluid with mirror quarter baffle cut is the optimum design condition for the STHE with maximum heat transfer rates and lower pressure drops.

Key words:

Cuo Nano fluid, Heat transfer, Pressure drop, Shell and tube heat exchanger.

1. INTRODUCTION:

Heat exchanger is a universal device in many industrial applications and energy conversion systems.

Various heat exchangers are designed for different industrial processes and applications. In heat exchangers, shell and tube heat exchanger presents great sustainability to meet requirements and gives efficient thermal performance. STHE are widely used in petro-chemical industry, Power generation, energy conservation and manufacturing industry [1]. The baffle member plays an important role in STHE and it supports tube bundle and also equally distribute the fluid in shell side. When segmental baffles are used in STHE which have many disadvantages [2-3]. The low heat transfer is achieved due to the flow stagnation i.e., dead zones which are created at the corners between baffle and shell wall [4]. It requires higher pumping power and it creates high pressure drop under the same heat load. The orientation of tubes will influence the annular surface area surrounded by the fluid. It is also influences the heat transfer rate.

New baffle cut arrangement is achieved higher heat transfer rates and lower pressure drops [5-8], so it is required to develop a new type STHE using different baffle cut arrangement to achieve higher heat transfer rate. The last few years which describe methods to calculate heat transfer and pressure drop in shell side of STHE with different baffles [9]. The different calculation procedures have been checked in against an experimental measurements on small scale heat exchanger. The Kern method, Tinker method and Delaware method [10-12] gave the best results. Compared with other methods in literature. The shell side design under the flow phenomenon inside the shell must be understood by experimental and numerical analysis.

The shell and tube heat exchanger design explained by Gay et al [13] worked on heat transfer, while Halle et al [14] Pekdemir et al investigated pressure drop [15-17]. Now a days the numerical methods have become an economical alternative for the research of STHE, through which detailed flow pattern and temperature field could be obtained with much less difficult [18-21]. In order to attain better performance characteristics (high heat transfer rates and low pressure drops) the STHE have to maintain the geometry of the heat exchanger and heat transfer fluids (Nano fluids [22]. Fluid which consisting of nano size particles is a Nano fluid and the fluid is dispersed in a conventional fluid. Basically used conventional fluids are water, engine oil, ethylene glycol have low thermal conductivity relative to metal and even metal oxides. The procedure for preparation of Nano fluid, factors such as the volume fraction, dimensions, shapes and properties of the nanoparticles are discussed by Yimin Xuan [23].

Saurabh Kumar [24] et.al and H.A.Mohammeda [25] et al. worked on different Nano fluids like Ag, SiO₂, CuO, TiO₂ and Al₂O₃ Nano fluids with different volume fractions (1-5%) to enhance the optimum heat transfer rate in the heat exchanger. P. C. Mukesh Kumar et al. [26] report on the heat transfer coefficient and pressure drop of a helically coiled tube heat exchanger handling Al₂O₃ nano fluid with water as base fluid. Here the volume concentration of nanoparticles is 0.1%, 0.4% and 0.8%. The Dean Number (De) range of 1650-2650 under laminar flow condition. According to Jaafar Albadr et al. [27] the volume concentration of the Al₂O₃ increases for the increase in heat transfer coefficient it causes the viscosity of nano fluid. S. Zeinali Heris et al. [28] Al₂O₃ nano particles dispersion in water fluid effects the heat transfer coefficient due to dispersion, chaotic movement of nanoparticles, Brownian motion and particle migration which leads to changes in thermal conductivity. The collective effect of all the above parameters on heat transfer is quite interesting to design STHE with the optimistic approach.

Baffle cuts are placed to increase the flow rate in shell side and also reduces the vibrations of shell and tube heat exchanger. A STHE with twelve copper tubes and stainless steel shell is considered for the proposed system. Numerical analysis is conducted with water and different concentrations i.e. 0.1%, 0.4%, 0.8% of CuO. The modifications in the shell side overall pressure loss in the shell from entrance to exit points of fluid is determined. The baffle cuts are provided at 25% with respect to the diameter and quarter baffle cut with respect to the cross sectional area, Mirror quarter baffle cut also considered for effective heat transfer. It is observed that, heat transfer rate increases with increase of surface area and increased concentration of Nano fluid.

2. NUMERICAL ANALYSIS AND VALIDATION OF THE WORK:

For the numerical analysis, the actual model is represented as a virtual computer model using CATIA software package and analysis is performed with finite volume method as a CFD tool. The inlet and outlet boundary conditions for the analysis is carried out as follows.

2.1 VOLUME CONCENTRATION ESTIMATION:

Thermo physical properties of Nano fluid are essential for the evaluation of heat transfer coefficient. These properties vary with concentration and temperature. The effect of variation of these parameters on thermo physical properties has been taken by Lee et al. [1998], Das et al. [2000], Xuan and Roetzel [2003], Pak and Cho [1998] and Choi et al. [2003]. Thermo physical properties of base fluid (CuO + water) are taken from ASHRAE HANDBOOK [1972]. For 40 nm diameter CuO Nano particle properties are

$$\rho = 6510 \text{ Kg/m}^3, c_p = 540 \text{ kJ/kg}^\circ\text{k} \text{ and } K = 18 \text{ w/m}^\circ\text{k}.$$

A) Density Calculation

$$\rho_{nf} = \phi \cdot \rho_p + (1 - \phi) (\rho_{bf}) - I$$

Where ρ_{nf} = Density of Nano fluid in Kg/m³,

ϕ = Concentration,

ρ_p = Density of Nano particle in Kg/m^3 ,

And ρ_{bf} = Density of base fluid in Kg/m^3 .

B) Specific Heat Calculation

$$C_{p_{nf}} \cdot \rho_{nf} = (1 - \phi) (\rho c)_w + \phi (\rho c)_p \text{ -II}$$

Where $C_{p_{nf}}$ = Specific heat of Nano fluid in $\text{KJ/kg}^\circ\text{k}$,

ρ_{nf} = Density of Nano fluid in Kg/m^3 ,

ϕ = Concentration,

$(\rho c)_w$ = Product of density and specific heat of water,

And $(\rho c)_p$ = Product of density and specific heat of Nano particle.

C) Viscosity Calculation

$$\frac{u_{nf}}{u_w} = \left(\left(1 + \frac{\phi}{100} \right)^{11.3} \left(1 + \left(\frac{T_{nf}}{70} \right) \right)^{-0.038} \left(1 + dp170 \right) - 0.061 \right) \text{ -III}$$

Where u_{nf} = Viscosity of Nano fluid in Kg/ms ,

u_w = Viscosity of base fluid in Kg/ms ,

ϕ = Concentration,

T_{nf} = Temperature of Nano fluid in $^\circ\text{C}$,

And d_p = Nano particle size in nm .

D) Thermal Conductivity Calculation

$$\frac{k_{nf}}{k_w} = 0.8938 \left(1 + \frac{\phi}{100} \right)^{1.37} \left(1 + \frac{T_{nf}}{70} \right)^{0.2777} \left(1 + dp150 \right) - 0.0336 (\alpha p \alpha w) 0.01737 \text{ -IV}$$

Where k_{nf} = Thermal conductivity of Nano fluid in $\text{w/m}^\circ\text{k}$,

k_w = Thermal conductivity of base fluid in $\text{w/m}^\circ\text{k}$,

ϕ = Concentration,

T_{nf} = Temperature of Nano fluid in $^\circ\text{C}$,

d_p = Nano particle size in nm ,

α_p = Thermal diffusivity of Nano particle in m^2/s ,

And α_w = Thermal diffusivity of Nano particle in m^2/s .

By using above equations I, II, III and IV, the properties of Nano fluids at different volume concentrations i.e. 0.1%, 0.4% and 0.8% are tabulated.

Table.1 Prorerties of Cuo Nano fluids at different concentrations.

%	ρ (kg/m^3)	K ($\text{w/m}^\circ\text{k}$)	μ (kg/ms)	C_p ($\text{J/kg}^\circ\text{k}$)
0.1	984.18 1	0.7615	0.000386 5	4167.8
0.4	1000.7 7	0.7647	0.000399 8	4096.9
0.8	1022.9 0	0.7689	0.000418 2	4006.6

2.2 INLET OUTLET AND BOUNDARY CONDITIONS FOR THE ANALYSIS OF SHELL AND TUBE HEAT EXCHANGER

2.2.1 Inlet and outlet conditions for hot fluid:

The different concentrations of Nano fluids and hot water are entered at a temperature of 345°k and different mass flow rates such as 0.16825kg/sec , 0.3871kg/sec , 0.5825kg/sec and 0.7691kg/sec are given for Cuo 0.1% Nano fluid, 0.1741kg/sec , 0.4004kg/sec , 0.6026kg/sec and 0.7956kg/sec are given for Cuo 0.4% Nano fluid and 0.1821kg/sec , 0.4188kg/sec , 0.63036kg/sec and 0.8322kg/sec are given for Cuo 0.8% Nano fluid at the inlet of heat exchanger tube side nozzle. From the tube flow is considered to atmosphere pressure only. Based on the given inlet and outlet conditions the inbuilt program of fluent software calculated remaining parameters.

2.2.2 Inlet and outlet conditions for cold fluid:

The cold fluid enters at a temperature of 300°k and different mass flow rates such as 0.3492kg/sec , 0.8031kg/sec , 1.2087kg/sec and 1.5958kg/sec are given at inlet of heat exchanger shell side nozzle. The flow of cold water is guided by the baffles provided over the tubes the water is entered at 300°k and atmospheric pressure and it is exited from the shell outer nozzle into atmospheric pressure. Hence the pressure boundary is defined at the outlet of the shell.

2.2.3 Other boundary conditions and grid generation:

No slip condition for tube shell inner and outer surfaces are given. Tube shell and inlet outlet nozzles with uniform cross sections are defined for the analysis. The direction of flow was defined normal to the boundary. Hydraulic diameter and turbulent intensity were specified at inlet nozzle of both hot and cold fluid. The flow is assumed as incompressible turbulent flow the gradient of temperature is required at all the points of the heat exchanger. Hence the grid generator for both tube and shell and they are separated by the boundaries.

2.3 NUMERICAL SOLUTION CHOSEN FOR THE ANALYSIS:

The CFD solver FLUENT was employed to solve the governing equations. The SIMPLE algorithm was used to resolve the coupling between pressure and velocity field. The second order upwind scheme was used for discretization pressure, momentum, energy, turbulent kinetic energy and turbulent dissipation rates. The analysis is related to fluid flow which is continuously shear hence the finite volume method which is flux based method is chosen for the analysis. In finite volume technique, Computational Fluid Dynamics (CFD) analysis there are three basic steps involved:

- 1) Integration of fluid governing differential equations over each control volume of computational domain.
- 2) Discretization of integrated equation into algebraic equation / form which will be converted into solution algorithm.
- 3) Control volume that will be solved in this discretized form equation will be used to write a solution algorithm for every iterative process until it satisfies the convergence criteria and stability

In Finite Volume Method (FVM) the domain can be divided into number of control volumes and place number of nodal points in between points as shown in Fig.4.

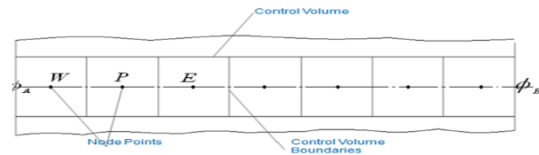


Figure .1 Nodal points in the flow domain

Discretization of Integrated equation into algebraic equation. The nodal point P is as shown in Fig.5.

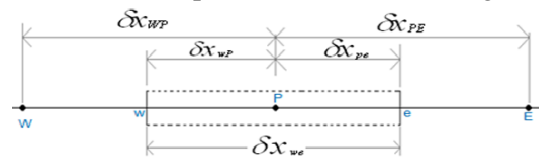


Figure .2 Control volume for FVM

The general equation for the fluid, when the fluid is incompressible, viscous, turbulent is

$$\int_{cv} \frac{\partial}{\partial t} (\rho\phi) dv + \int_{cv} \text{div}(\rho\phi u) dv = \int_{cv} \text{div}(\Gamma \text{grad}\phi) dv + \int_{cv} S(\phi) dv - V$$

Where ϕ = Property of fluid.

ρ = Density of fluid.

Γ = Diffusion coefficient.

S = source term.

The general transport equation for a variable ϕ in finite volume method is

(Rate of increase of ϕ of fluid element) + (Net Rate of fluid flow of ϕ out of fluid element) = (Rate of increase of ϕ due to diffusion) + (Rate of increase of ϕ due to source)

$$a_p \phi_p = a_w \phi_w + a_e \phi_e + S_u - V I$$

Where $a_w = \frac{\Gamma_w A_w}{\delta x_{wp}}$, $a_e = \frac{\Gamma_e A_e}{\delta x_{pe}}$ & $a_p = (a_w + a_e - S_p)$

The resulting system of linear algebraic equations is then solved to obtain the distribution of the property ϕ at the nodal point. The algebraic equations are solved by using direct methods (Cramer’s rule, matrix inversion and Gauss elimination) and indirect or iterative methods (Jacobi and Gauss-seidel). The flow is incompressible turbulent hence the k-ε model is considered for the analysis. K-ε model is simplest turbulence model for which only initial boundary conditions need to be supplied and used for 3D analysis in which the changes in the flow direction are always so slow that the turbulence can adjust itself to local conditions.

As per the grid density the number of algebraic equations are generated for unite volume the algebraic equations are solved by numerically.

3 VALIDATION OF THE ANALYSIS

The above boundary conditions, inlet and outlet conditions and fluid properties are considered for the analysis and the results are compared with real model. The virtual model of shell and tube heat exchanger is used for numerical analysis as shown in Fig.6. Fig.7 and Fig.8 show the variations of heat transfer in shell side and tube side of shell and tube heat exchanger in vector form. The problem has taken from “NUMERICAL AND HEAT TRANSFER ANALYSIS OF SHELL AND TUBE HEAT EXCHANGER WITH CIRCULAR AND ELLIPTICAL TUBES” J. Bala Bhaskara Rao, V. Ramachandra Raju. Consequently experimental results are approached to numerical results and the final concept is formulated towards CFD analysis for various configurations.

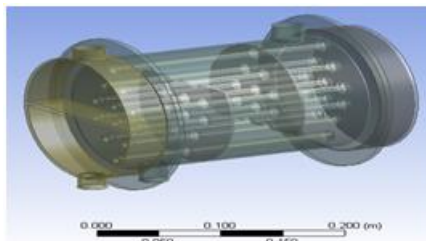


Figure.3 Virtual model of heat exchanger

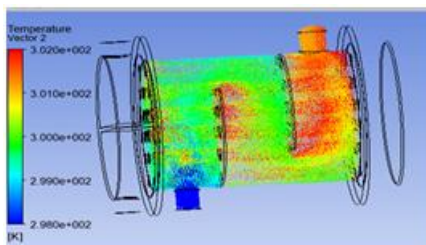


Figure.4 Shell side vector diagram of heat transfer

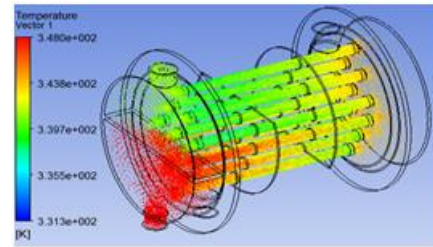


Figure.5 Tube side vector diagram of heat transfer

4. DATA APPRECIATION

The heat transfer rate and ultimately pressure drop was calculated from the initial data on the flow rates and the inlet and outlet temperatures of both shell and tube side of STHE. The heat transfer rate is obtained by the following equation.

$$Q = AU\Delta T_m \quad (1)$$

Where Q=average heat flux between the cold and hot fluid in watts

$$Q = (Q_c + Q_h) / 2$$

$$Q_c = m_c c_{pc} (T_{co} - T_{ci})$$

$$Q_h = m_h c_{ph} (T_{hi} - T_{ho})$$

m_c, m_h are cold and hot fluid mass flow rates in kg/sec. C_{pc}, c_{ph} are specific heats under constant pressure of cold and hot fluids in kj/kg k.

5 RESULTS & DISCUSSION

The flow parameters are varied by introducing of different concentrations of Nano fluids in tube side and different baffle cuts. Subsequently more heat transfer rate is created in the flow by introducing more surface area and mathematical model is reformed for more numerical analysis. Observations as per this type of analysis found more heat transferefficiency for dropping the pressures along the length of shell and tube of STHE.

5.1 HEAT TRANSFER ANALYSIS

5.1.1 Heat transfer with different baffle cuts

In this experiment three types of baffle cuts are used for the analysis. The effect of heat transfer in tube side and shell side are investigated by using 25% baffle cut, quarter baffle cut and mirror quarter baffle cut.

The streamline contours in mathematical model shown in Fig.10, Fig.11, Fig.12 and Fig.13 for Cu₀ 0.8% concentration Nano fluid indicates heat transfer distribution in tube side and shell side of shell and tube heat exchanger. The temperature of the hot water in the tubes at the inlet is higher than all other regions. In the case of shell the temperature of cold water at the outlet is higher. From all graphs it shows heat transfer rate increases with increase of Reynolds number. The baffle cut changes the direction of the flow of cold fluid and increases the heat transfer rate due to increase of surface area. The heat transfer rate increases from 25% baffle cut to quarter baffle cut and also quarter baffle cut to mirror quarter baffle cut.

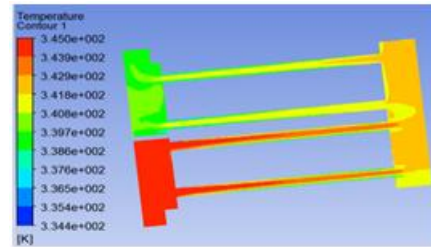


Figure.9 Tube side temperature contour at mirror quarter baffle cut

In the case of quarter baffle cut the direction of flow of cold fluid changes in X-Y plane and also in Z direction. As a result the total length of flow increased and heat transfer rate also proportionately increase. The heat transfer rate increases up to 8% when the 25% baffle cut is replaced by quarter baffle cut (90 baffle cut) and it is up to 20% when quarter baffle cut is replaced by mirror quarter baffle cut for water as a working fluid in tube side and shell side of STHE from Fig.14. This is due to increase flow length in Z direction for quarter baffle cut. In the case of mirror quarter baffle cut (M90 baffle cut) the flow of cold fluid split in to two streams and follows the helical path due to baffle shape. Separation of cold fluid and increase in flow length leads to a better heat transfer rate. The heat transfer rate increases up to 18%, 20% and 28% when the 25% baffle cut is replaced by quarter baffle cut for Cu₀ as a working fluid in tube side with 0.1%, 0.4% and 0.8% concentrations respectively from Fig.15, Fig.16 and Fig.17. When quarter baffle cut is replaced by mirror quarter baffle cut the heat transfer rate increases up to 25%, 20% and 27% for Cu₀ as a working fluid in tube side with 0.1%, 0.4% and 0.8% concentrations respectively from Fig.15, Fig.16 and Fig.17.

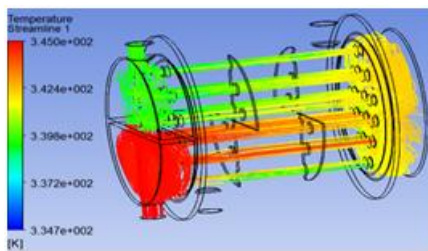


Figure.6 Streamlines of tube side heat transfer at mirror quarter baffle cut

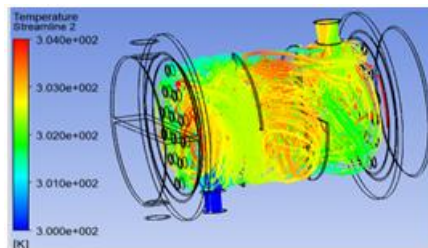


Figure.7 Streamlines of shell side heat transfer at mirror quarter baffle cut

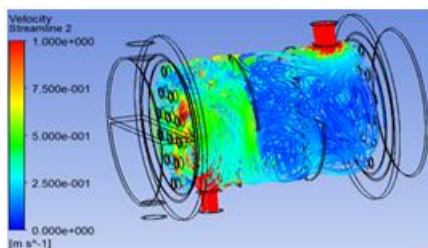


Figure.8 Streamlines of shell side velocity at mirror quarter baffle cut

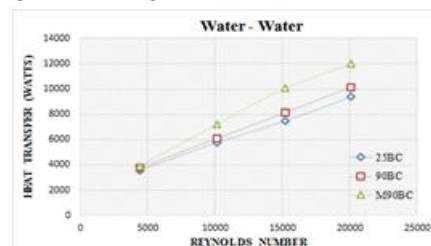


Figure.10 Heat transfer at different baffle cuts with water as working fluid in tube side.

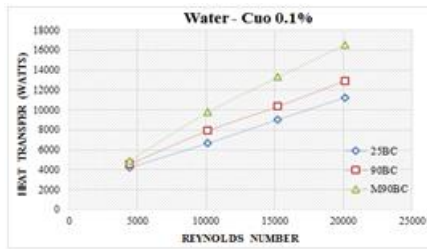


Figure.11 Heat transfer at different baffle cuts with CuO 0.1% as working fluid in tube side

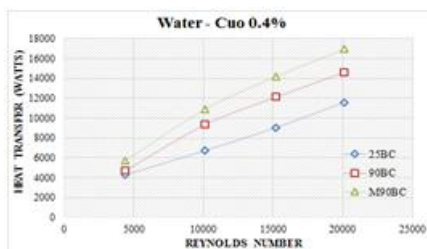


Figure.12 Heat transfer at different baffle cuts with CuO 0.4% as working fluid in tube side

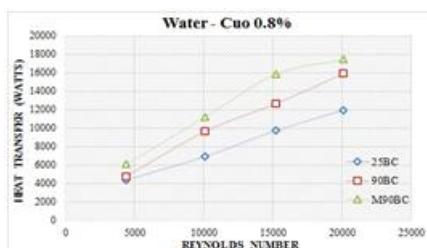


Figure.13 Heat transfer at different baffle cuts with CuO 0.8 % as working fluid in tube side

5.1.2 Heat transfer with different CuO concentration Nano fluids

Analysis for heat transfer rate with different concentrations of CuO Nano fluid to water at individual baffle cuts namely 25% baffle cut, quarter baffle cut and mirror quarter baffle cut. The heat transfer rate for CuO 0.1% concentration to water at 25% baffle cut is observed as 20%. The temperature difference between hot fluid and cold fluid influences the heat transfer rate. While different concentrations of CuO Nano fluid i.e. 0.4% and 0.8% to water transformations noticed the heat transfer rate as 25% and 29% respectively for the 25% baffle cut. Similarly at quarter baffle cut and mirror quarter baffle cut the heat transfer rate is increased 24%, 40%, 48% and

27%, 45%, 49% respectively for the above mentioned different concentrations of nano fluid to water. From all the graphs in Fig.18, Fig.19 and Fig.20 values imposes heat transfer rate increases from 0.1% concentration to 0.8% concentration of CuO Nano fluid.

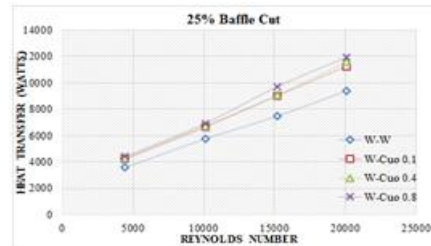


Figure.14 Heat transfer at different working fluids with 25% baffle cut

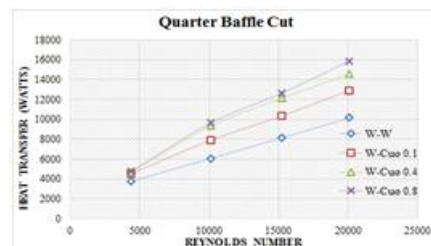


Figure.15 Heat transfer at different working fluids with quarter baffle cut



Figure.16 Heat transfer at different working fluids with mirror quarter baffle cut

5.2 PRESSURE DROP ANALYSIS:

For a fluid flow pressure, volume, temperature of the three inter dependent parameters. The heat transfer is high when the temperature difference in between hot and cold fluid is more and pressure drop also high. But in the case of heat exchanger a sudden high pressure drops are not encourage. To avoid high pressure drop in the heat exchanger a uniform transfer of heat energy through the heat exchanger is required.

With this view the pressure drop with different arrangements is calculated for the better performance of the heat exchanger.

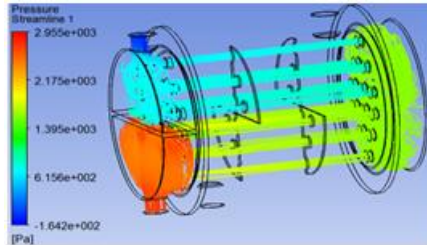


Figure.17 Stream lines of tube side pressure drop at mirror quarter baffle cut

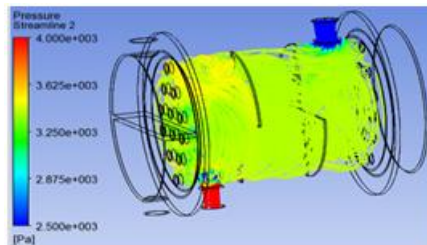


Figure.18 Streamlines of shell side pressure drop at mirror quarter baffle cut

5.2.1. Shell side Pressure drop with different baffle cuts:

The baffle cuts influences the direction of flow of cold fluid and baffles gives structural support to the tubes. The streamline contours in mathematical model shown in Fig.21 and Fig.22 indicates pressure drop variation in tube side and shell side of shell and tube heat exchanger. The pressure drop increases with increase of Reynolds number. The pressure drop decreases from 25% baffle cut to quarter baffle cut and also quarter baffle cut to mirror quarter baffle cut. The total length of flow increases in quarter baffle cut as compare to 25% baffle cut and it leads to decrease the pressure drop in shell side of shell and tube heat exchanger. The pressure drop reduced up to 10% for quarter baffle cut as compared to 25% baffle cut as shown in Fig.28. In case of mirror baffle cut the fluid in shell split into two streams, increase the flow path and reduce the pressure drop in shell side. The pressure drop reduced up to 20% form quarter baffle cut to mirror quarter baffle cut as shown in Fig.28.

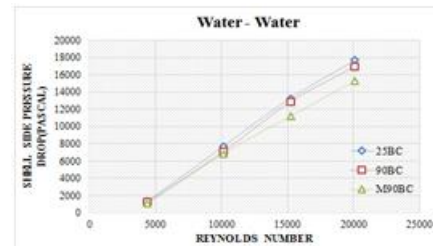


Figure.19 Shell side pressure drop at different baffle cuts with water as hot fluid

5.1.3. Tube side pressure drop on shell and tube heat exchanger:

The influence of pressure drop along tube side of shell and tube heat exchanger with different concentrations of Nano fluids is calculated. The pressure drop for water to water transformation is 12% from 255 baffle cut to quarter baffle cut whereas the same observation for mirror baffle cut to quarter baffle cut is 18%. Now using different concentrations i.e. 0.1%, 0.4% and 0.8% of CuO Nano fluids with water, the pressure drop is 15%, 17% and 16% for 25% baffle cut to quarter baffle cut and also 16%, 15% and 12% for quarter baffle cut to mirror quarter baffle cut respectively from Fig.23, Fig.24 Fig.25 and Fig.26. The pressure drop is observed as minimum for mirror quarter baffle cut and the percentages are increased namely 14%, 23% and 30% at 0.1%.0.4% and 0.8% concentration of CuO Nano fluid with water respectively.

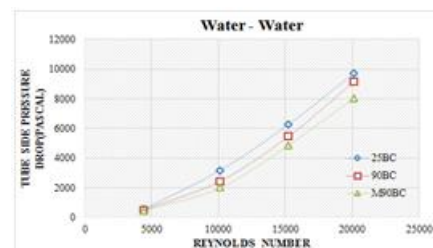


Figure.20 Tube side pressure drop at different baffle cuts with water as hot fluid

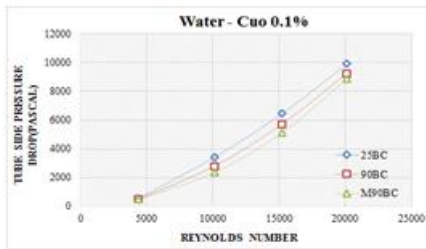


Figure.21 Tube side pressure drop at different baffle cuts with CuO 0.1 as hot fluid

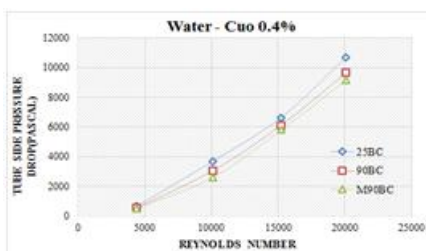


Figure.22 Tube side pressure drop at different baffle cuts with CuO 0.4 as hot fluid

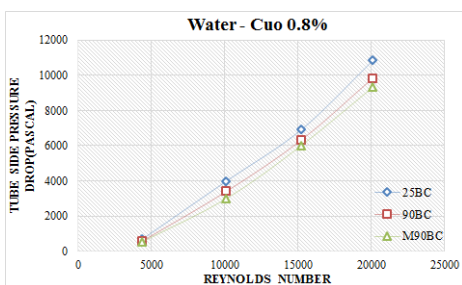


Figure.23 Tube side pressure drop at different baffle cuts with CuO 0.8 as hot fluid

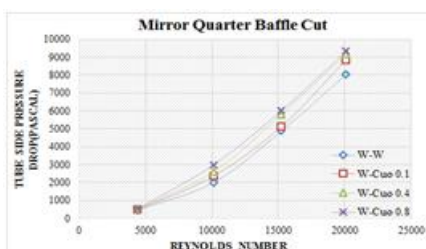


Figure.24 Tube side pressure drop at different working fluids with mirror quarter baffle cut

6. CONCLUSIONS:

In the present study numerical analysis is carried out on the heat transfer behavior of Nano fluids through STHE under turbulent flow conditions with various

baffle cuts. CuO/water with different concentrations are used to enhance the heat transfer rate by minimizing the pressure drop. Based on the simulation results following conclusions are derived.

- The overall heat transfer rate in the Reynolds number range between 4000 to 20000 increases with mirror baffle cut at CuO 0.8% concentration with water is 30% higher than existing shell and tube heat exchanger.
- Pressure drop reduction in shell side is more influenced by baffle cuts. The pressure drop is minimum in the case of mirror quarter baffle cut and it is 20% less as compared to 25% baffle cut.
- The pressure drop in tube side increases against increase in concentrations of CuO Nano fluid and it is maximum for 0.8% CuO with water.

7. REFERENCES:

- Qian SW (2002) Handbook for heat exchanger design. Chemical Industry Press, Beijing (in Chinese)
- D.Q. Kern, Process Heat Transfer, Mc-Graw-Hill, New York, 1950, pp. 127–171.
- H.D.Li, V.Kottke, effect of leakage on pressure drop and global heat transfer in shell and tube heat exchanger for staggered tube arrangement, Int.J.Heat Mass Transfer 41 (2) (1998) 425-433.
- H.D.Li, V.Kottke visualization and determination of local heat transfer coefficient in shell and tube heat exchangers for staggered tube arrangement by mass transfer measurements. Exp.Therm. Fluid sci. 17 (3) (1998) 210-216.
- B.I.Master, K.S.Chunangad, A.J.Boxma, D.Kral, P.Stehlik, most frequently used heat exchangers from pioneering research to world wide applications, heat transfer Eng. 27 (6) (2006) 4-11.
- Mukherjee R (1992) Use double-segmental baffles in the shell-and-tube heat exchangers. Chem Engg Prog 88:47-52.

7. Li H, Kottke V (1998) effect of baffle spacing on pressure drop and local heat transfer in shell and tube heat exchangers for staggered tube arrangement. *Int J Heat Mass Transfer* 41(10):1303-1311.
8. Lei YG He YL, Pan C et al (2008) design and optimization of heat exchangers with helical baffles *Chem Engg Sci* 63(17):4386-4395.
9. Peng B, Wang QW, Zhang C et al 2007 and experimental study of shell and tube heat exchanger with continuous helical baffles. *J Heat transfer* 129:1425-1431.
10. J.W. palen and J. Taborek, Solutions of shell side flow pressure drop and heat transfer by stream analysis method, *Chem. Eng. Progr. Symp. Series*, 65(1969) 53-63.
11. D.Q. Kern, *Process Heat transfer*, McGraw-Hill, New York, 1950.
12. T. Tinker, shell side characteristics of shell and tube heat exchangers, Part I, II, III, *General Discussion on Heat Transfer Inst. Mech. Eng.*, London 1951, PP. 97-116.
13. K.J. Bell, *Final Report of the Cooperative Research Programme on Shell and Tube Heat Exchangers*, University of Delaware, Engineering Experimental Station, Bulletin No. 5, 1963.
14. Gay B, Mackely NV, Jenkins JD. Shell-side heat transfer in baffled cylindrical shell-and-tube exchangers-an electro chemical mass transfer modelling technique. *Int J Heat mass transfer* 1976:19:995-1002.
15. Halle H, Chenoweth JM, Wabsganss MW. Shell side water flow pressure drop distribution measurements in and industrial sized test heat exchanger. *J Heat mass transfer* 1988:110:60-7.
16. Pekdemir T, Davies TW, Haseler LE, Diaper AD. Pressure drop measurements on the shell side of a cylindrical shell and tube heat exchanger. *Heat Transfer Eng.* 1994:15:42-56.
17. Li HD, Kottke V, visualization and determination of local heat transfer coefficient in shell and tube heat exchangers for staggered tube arrangement by mass transfer measurements. *Exp Therm fluid Sci:* 1998:17:210-6.
18. Seemawute P, Eiamsa-ard S. thermo hydraulics of turbulent flow threw a round tube by a peripheral-cut twisted tape with an alternate axes international communications in heat and mass transfer 2010:37:652-9.
19. D.B. Rhodes, L.N. Carlucci, predicted and measured velocity distributions in a model heat exchanger, In: *Int. Conf. on numerical methods in engineering Canadian nuclear society/American nuclear society* 1983, PP. 935-948.
20. X. Huang, Z. Lu, Wang, numerical modelling of the shell side flow in the shell and tube heat exchanger in: W. Liu ed, *proc. Int. conf. on energy Conversion and application volume I*, Wuhan, china 2001, PP 301-304.
21. Z. Stevanovic, G. Ilic, N. Radojkovic, M. Vukic, V. Stefanovic, G. Vuckovic, design of shell and tube heat exchanger by using CFD Technique-Part one: Thermo Hydraulic calculations, *Mechanical Engineering* 1 (8) (2001) 1091-1105.
22. Mr. Vatsal. S. Patel et al (2013) An Experimental Study of Counter flow Concentric Tube Heat Exchanger using CuO / Water Nano fluid.
23. Yimin Xuan, Qiang Li Heat transfer enhancement of Nano fluids *International Journal of Heat and Fluid Flow* 21 (2000) 58-64.



24. Saurabh Kumar et al (2015) Computational Analysis of Different Nano fluids effect on Convective Heat Transfer Enhancement of Double Tube Helical Heat Exchanger.
25. H.A. Mohammed Numerical study of heat transfer enhancement of counter nano fluids flow in rectangular micro channel heat exchanger, Super lattices and Microstructures 50 (2011) 215-233.
26. P. C. Mukesh Kumar et al CFD analysis of heat transfer and pressure drop in helically coiled heat exchangers using Al₂O₃ / water nano fluid, Journal of Mechanical Science and Technology 29 (2) (2015) 697-705.
27. Jaafar Albadr et al Heat transfer through heat exchanger using Al₂O₃ nano fluid at different concentrations , case studies in thermal engineering 1(2013) 38-44.
28. S. Zeinali Heris Experimental investigation of convective heat transfer of Al₂O₃/water nano fluid in circular tube, International Journal of Heat and Fluid Flow 28 (2007) 203–21.